Dynamic terahertz polarization in single-walled carbon nanotubes

X. L. Xu, P. Parkinson, K.-C. Chuang, M. B. Johnston, R. J. Nicholas, and L. M. Herz
Clarendon Laboratory, University of Oxford, Parks Road, Oxford OX1 3PU, United Kingdom
(Received 1 July 2010; revised manuscript received 23 July 2010; published 24 August 2010)

We have investigated the anisotropic dynamic dielectric response of aligned and well-isolated single-walled carbon nanotubes using optical-pump terahertz (THz)-probe techniques. The polarization anisotropy measurements demonstrate that the THz radiation interacts only with radiation polarized parallel to the nanotubes which have been selectively excited by a polarized pump pulse thus allowing controlled THz polarization to be achieved from unaligned nanotubes.

DOI: 10.1103/PhysRevB.82.085441 PACS number(s): 78.47.−p, 72.80.Rj, 78.67.Ch, 73.63.Fg

Single-walled carbon nanotubes (SWNTs) have attracted much attention owing to their striking chemical and physical properties[1] and their potential applications in nanoelectrics and biosensors.[1–3] Like other low-dimensional materials, including organic polymers, organic small molecular crystals, or quantum dot chains,[4–6] this quasi-one-dimensional material has intrinsically anisotropic physical properties. Anisotropy in the dielectric properties of SWNTs at visible and near-infrared frequencies has recently attracted much attention[7–11] and aligned SWNTs have been shown to act as effective terahertz (THz) polarizers.[12] An understanding of *transient* anisotropy in the dielectric response in SWNTs is of importance for the design of new ultrafast devices.

Current high-speed devices based on inorganic semiconductor technology are limited to operating at frequencies below ~100 GHz. Technologies based on SWNTs have the potential to revolutionize high-speed optoelectronic devices and achieve operating frequencies in the THz band. Therefore it is important to characterize the electrical and optical properties of SWNTs at THz frequencies. Optical pump THz probe spectroscopy (OPTPS) is an ideal tool for investigating such materials. The technique can be used to measure the complex dielectric response of a material over a wide frequency band on picosecond time scales after optical excitation.

The anisotropic optical response of SWNTs has been studied previously both theoretically[13] and experimentally; techniques used have included Raman scattering, UV-visible absorption, fluorescence, far-infrared spectroscopy, THz-time-domain spectroscopy, and pump-probe spectroscopy.[7–10,12,14–16] However, there has been limited success in elucidating the intrinsically transient anisotropic response of SWNTs. Two main factors have impeded such an investigation. First, there is a strong tube-tube interaction that exists in the bundled nanotubes and introduces a subpicosecond carrier decay channel,[17–19] which smears out the intrinsically ultrafast dynamic response. In many respects this problem has been solved by the development of new methods, such as those by Bachilo *et al.*,[20] to prepare SWNTs so that they are effectively isolated from each other. Second, it is difficult to produce samples of macroscopic size that contain aligned SWNTs. Recently Kim *et al.*[9] have solved this problem by using a stretching technique to create well-aligned free-standing SWNT-gelatin films.

In this report the dielectric response of stretch-aligned, well-isolated SWNTs has been investigated using OPTPS. We measure the polarization anisotropy of the dielectric response by adjusting the polarization of a near-infrared ($\lambda \simeq 800$ nm) "pump" pulse and that of a single-cycle THz "probe" pulse ($\lambda \sim 300$ μm). The transient anisotropy is measured by adjusting the delay between the optical pump and the THz probe pulses.

SWNTs grown by high-pressure carbon monoxide were purchased from Carbon Nanotechnologies. SWNTs were isolated using ultracentrifugation and sonication according to the technique described in Ref. 20. Gelatin was used as a matrix to wrap SWNTs and prevent reaggregation of SWNTs. Free-standing SWNT-gelatin films were then stretched with a ratio of ~2.5 using the method presented by Kim *et al.*[9] The thickness of the sample presented in this paper was $L=0.059\pm0.002$ mm. A detailed description of our OPTPS setup can be founded elsewhere.[21]

To obtain a quantitative information on anisotropic response, we consider the imperfect alignment of SWNTs in the samples with the method by Hashimoto *et al.*[22] The nematic order parameter S is used where S_1 is the proportion of SWNTs well aligned along the stretched axis and S_2 is the proportion aligned perpendicular to the stretched SWNTs axis and $S_1+S_2=1$. The mixed alignment leads to the four possible measurement configurations shown in Fig. 1. It is noted that instead of rotating the polarization of THz, we rotate the SWNTs sample. The photon energy of the pump was tuned to the E_{22} exciton singularity of the SWNTs (1.55 eV), which can predominantly select (9,7), (10,5), and (11,3) semiconducting nanotubes.

The dielectric response of our SWNTs sample in the ab-

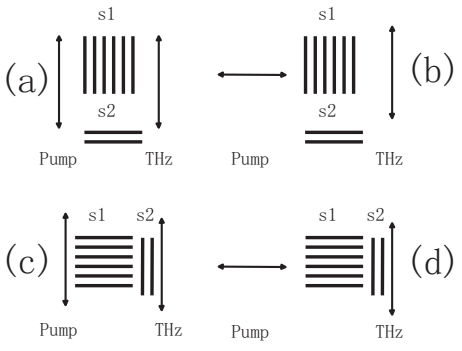

FIG. 1. Experimental schematic of the four different pump-probe polarization configurations used in the experiment.

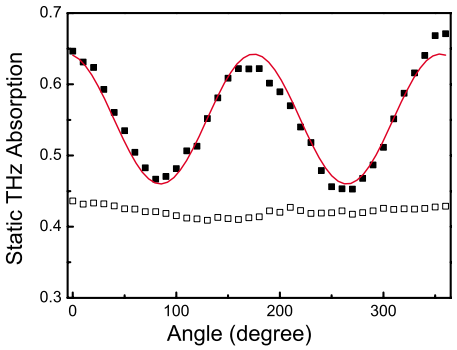

FIG. 2. (Color online) Dependence of static THz absorption (solid squares) as a function of angle between THz-wave polarization and the stretched axis with 0° corresponding to parallel case as shown in Fig. 1(a) and 90° corresponding to perpendicular case as shown in Fig. 1(c). The solid line is a fitting curve. Blank squares are the data for unaligned SWNTs.

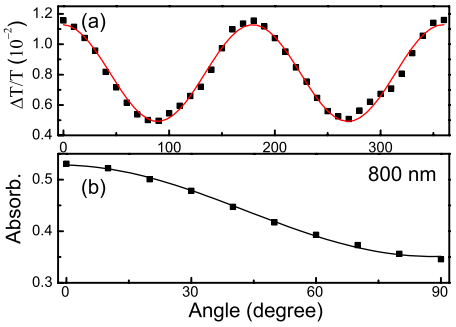

FIG. 3. (Color online) (a) Dependence of the optically induced differential transmission (solid squares) as a function of angle between THz-wave polarization and the stretched SWNTs axis while keeping pump polarization parallel to the stretched SWNTs axis. Here 0° corresponds to the parallel case shown in Fig. 1(a) and 90° corresponds to the perpendicular case as shown in Fig. 1(d). The solid line is a fitting curve. (b) Absorption anisotropy measured at 800 nm.

sence of the 1.55 eV pump photons (i.e., "in the dark") is shown in Fig. 2 as a function of the angle between the stretched axis of the SWNTs and the THz electric field. The angle of 0° corresponds to the THz polarization parallel to the *S*1 direction of the SWNTs sample as shown in Fig. 1(a). The integrated absorption coefficient of the sample at THz frequencies is plotted, $\alpha=-\ln(T/T_0)$, where T and T_0 are the transmission with and without sample, respectively. Control experiments were also conducted on unstretched samples as shown in Fig. 2 (blank squares). Within experimental uncertainty no polarization anisotropy could be observed.

Considering SWNTs as having a dipole moment μ_{xx} parallel to the SWNT axis, μ_{yy} perpendicular, and a diagonal dipole moment μ_{xy}, the polarized absorption by all dipoles as a function of angle can be expressed as $A=\mu_{xx}\cos^2\theta+\mu_{yy}\sin^2\theta+\mu_{xy}\sin 2\theta$,[5] shown as a fitting curve in Fig. 2. Our best fit parameters are $\mu_{xx}=0.641\pm0.004$ and $\mu_{yy}=0.461\pm0.004$, which are much larger than $\mu_{xy}=-0.017\pm0.003$, suggesting the dominant role of perpendicular and parallel dipole moments. The polarization ratio for the sample was found to be $\zeta=(\mu_{xx}-\mu_{yy})/(\mu_{xx}+\mu_{yy})=0.163$, which is relatively small, probably due to the relatively small stretching ratio.

A spectral analysis of the static dielectric function of our sample revealed that the response was Drude type. This indicates that the angular-dependent absorption displayed in Fig. 2 originates primarily from free carrier absorption of THz radiation. In the absence of photoinjection, mobile carriers are provided by metallic and thermally excited narrow-gap quasimetallic nanotubes or unintentional ambient oxygen doping in semiconducting SWNTs.[23] Therefore, these results may be explained by free carriers in the aligned nanotubes acting as a linear polarizer for THz radiation, in much the same way as a conventional wire grid polarizer functions.[12]

We now discuss the changes in the dielectric response of SWNTs that occur during and after photoexcitation. As mentioned above, photons with an energy of 1.55 eV have been shown by photoluminescence emission spectroscopy to resonantly pump the (9,7), (10,5), and (11,3) semiconducting SWNTs.[24,25] We have measured the change in the THz dielectric response of the stretch-aligned SWNTs as a result of photoexcitation. The dielectric response was monitored by measuring the differential transmission of THz radiation, $-(T_{on}-T_{off})/T_{off}=\delta T/T_0$, through the sample. Here T_{on} and T_{off} represent the transmission of the peak amplitude of a THz pulse through the photoexcited and unexcited samples, respectively. Since OPTPS measurements record only the *change* in the dielectric response resulting from photoexcitation, they thus ignore the "dark" response described above. Therefore, as the change in transmission (or absorption) of THz radiation is dominated by the photoinduced creation of excitons, the experimental results presented in Figs. 3 and 4 primarily describe the response of the *semiconducting* rather than the metallic SWNTs in our sample. Our previous studies have suggested that this is mainly an excitonic response rather than one from free carriers.[25]

Figure 3(a) shows how the "optical pump"-induced change in THz transmission, $\delta T/T_0$, varies as a function of the angle between the stretched axis of the SWNTs and the (linear) polarization of the THz probe, while keeping the pump polarization parallel to the stretched SWNTs axis. The data were acquired immediately after photoexcitation with the 1.55eV, 210 μJ cm^{-2} pump pulse. Fitting the data in Fig. 3 gives $\mu_{xx}=0.0113\pm0.0001$ and $\mu_{yy}=0.0049\pm0.0001$ and an essentially negligible $\mu_{xy}=(-9\pm7)\times10^{-5}$. The light-induced polarization ratio extracted from the data shown in Fig. 3 is $\zeta_{h\nu}=0.393$, which is clearly much larger than observed for the nonphotoexcited pulse. This is due to the strongly polarized absorption of SWNTs (Refs. 8 and 26) which preferentially selects SWNTs aligned parallel to the excitation polarization direction and gives rise to an enhanced transient anisotropy which has been shown to exist even in unaligned samples.[27,28]

In order to assess the degree of alignment of the semiconducting SWNTs, we measure the angular dependence of the absorption at 800 nm as shown in Fig. 3(b). This gives a polarization ratio $\zeta\simeq0.201$, which is comparable to that found for the unpumped THz response. We use this to estimate the values of S_1 and S_2. Using a value of $\alpha_\perp/\alpha_\parallel$ at 800

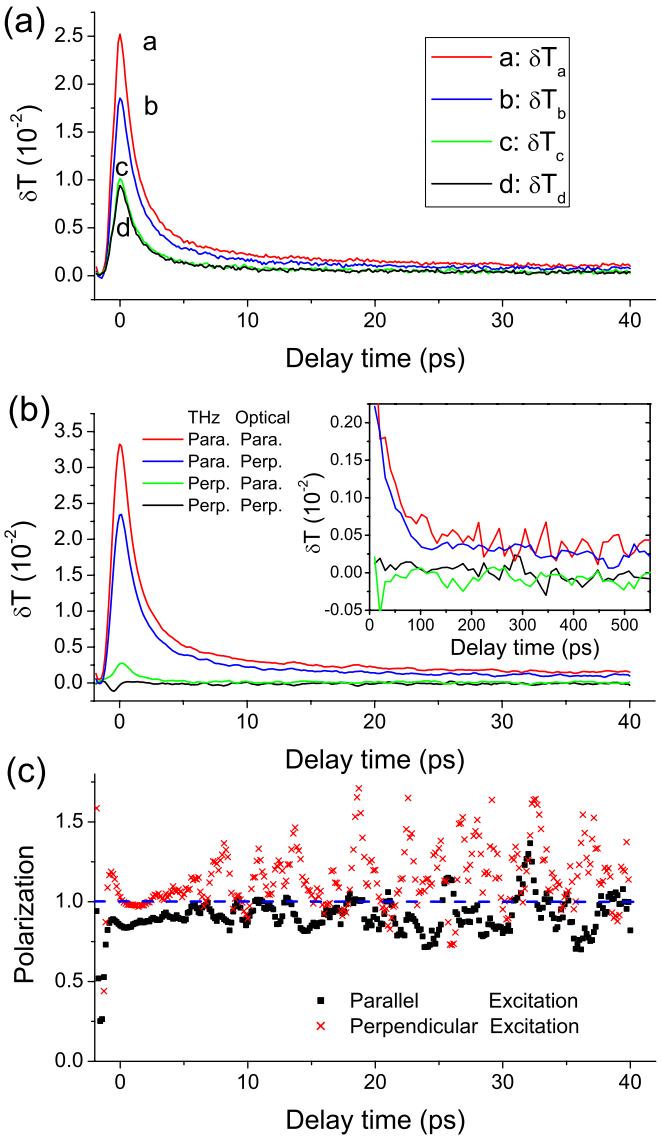

FIG. 4. (Color online) (a) Ultrafast responses for different pump-probe configurations corresponding to the four different pump-probe polarization configurations in Fig. 1. (b) Ultrafast responses deduced for optical and THz fields aligned precisely parallel and perpendicular to the nanotube axes as described in the text. The inset shows the longer time length dynamic responses. (c) Transient polarization as a function of time after photoexcitation for the pump polarization parallel (red) $P_{\|}$ and perpendicular (black) $P_{\perp}$ to the axis of the SWNTs.

nm of 0.32 as reported by Islam *et al.*,[26] gives S_1 (S_2) of approximately 0.71 (0.29).

We now discuss the time-resolved polarization and THz response of the semiconducting SWNTs. While the results displayed in Fig. 3 were obtained immediately after photoexcitation, Fig. 4 illustrates how the dielectric response changes with time and gives information on the exciton dynamics. Figure 4(a) shows the optically induced differential transmission of THz radiation measured in the four pump-probe polarization configurations shown in Fig. 1 under a fluence of ~210 μJ/cm^2. For all geometries shown the decay in $\delta T/T_0$ was of a multiple exponential form with a fast decay occurring over several picoseconds [Fig. 4(a)] and a much slower decay over hundreds of picoseconds [inset in Fig. 4(a)]. Our observations are consistent with decay dynamics reported using other techniques[17,22,28–30] and our previously reported results on similar unstretched films[25] all of which suggest that the initial decay is due to fast Auger recombination followed by a longer decay of single excitons.

We determine the response for fully aligned nanotubes by analyzing the mixed alignment using the parameters S_1 and S_2 which leads to the following four equations for the four different differential transmission measurement configurations as shown in Fig. 1:

$$\delta T_a = S_1 \delta T_{probe\|pump\|} + S_2 \delta T_{probe\perp pump\perp}, \quad (1)$$

$$\delta T_b = S_1 \delta T_{probe\|pump\perp} + S_2 \delta T_{probe\perp pump\|}, \quad (2)$$

$$\delta T_c = S_1 \delta T_{probe\perp pump\perp} + S_2 \delta T_{probe\|pump\|}, \quad (3)$$

$$\delta T_d = S_1 \delta T_{probe\perp pump\|} + S_2 \delta T_{probe\|pump\perp}, \quad (4)$$

where δT_a, δT_b, δT_c, and δT_d are the experimental data for the four configurations shown in Fig. 1, for example, $\delta T_{probe\|pump\|}$ is the corresponding data for THz and optical fields aligned perfectly relative to the nanotube axis. The resulting behavior deduced for the fully aligned responses are shown in Fig. 4(b). In practice there is some uncertainty in the final values (~10%) since there is significant error in the determination of S_1 due to both experimental uncertainties such as alignment changes on sample rotation and differences in the reported values for $\alpha_{\perp}/\alpha_{\|}$,[7,8,26] however, the main conclusion is that the THz response is essentially zero when polarized perpendicular to the nanotubes. This can be demonstrated by plotting the THz polarization as shown in Fig. 4(c) for optical excitation either parallel or perpendicular to the nanotubes as defined by

$$P_{\|} = \frac{\delta T_{probe\|pump\|} - \delta T_{probe\perp pump\|}}{\delta T_{probe\|pump\|} + \delta T_{probe\perp pump\|}}, \quad (5)$$

$$P_{\perp} = \frac{\delta T_{probe\|pump\perp} - \delta T_{probe\perp pump\perp}}{\delta T_{probe\|pump\perp} + \delta T_{probe\perp pump\perp}}, \quad (6)$$

The results indicate that within experimental error the response remains completely polarized for the entire period of the excitation pulse and no detectable THz absorption can be measured for radiation polarized perpendicular to the nanotubes. This conclusion is similar to that reported recently by Ren *et al.*[12] who found that highly aligned films of mechanically aligned, bundled films of nanotubes could act as highly effective THz polarizers and also showed no detectable THz response for the perpendicular configuration. In their case the response is fixed by the alignment of the tubes and attributed to the presence of free carriers which may be in either metallic or semiconducting tube. In our case the dynamic response comes from excitons which have been photoexcited into isolated semiconducting tubes with a polarization direction determined by the polarization of the pump pulse. This suggests that the absence of perpendicular THz response up to frequencies of ~2 THz is a very general property of car-

bon nanotubes and that they can function as a dynamic THz polarizer as a result of the induced absorption parallel to the pump pulse.

To conclude, we have studied the dynamic dielectric response of partially aligned single-walled carbon nanotubes embedded in gelatin using OPTPS. In the absence of photoexcitation the system acted as a weak THz polarizer with response due to metallic SWNTs or unintentional doping in semiconducting SWNTs. Using polarized photoexcitation, a large light-induced anisotropy is seen, which originates from selectively excited semiconducting nanotubes. No detectable THz response is seen for THz fields polarized perpendicular to the nanotubes throughout the duration of the excitation pulse. This shows that a randomly aligned film of nanotubes can be used to control the THz polarization directly by adjusting the polarization of the initial pump pulse.

This work was supported by the EPSRC.

[1] R. Saito, G. Dresselhaus, and M. S. Dresselhaus, *Physical Properties of Carbon Nanotubes* (Imperial College Press, London, 1999).
[2] J. Wang, Electroanalysis **17**, 7 (2005).
[3] R. H. Baughman and A. A. Zakhidov, Science **297**, 787 (2002).
[4] L. M. Herz and R. T. Phillips, Phys. Rev. B **61**, 13691 (2000).
[5] O. Ostroverkhova, D. G. Cooke, F. A. Hegmann, R. R. Tykwinski, S. R. Parkin, and J. E. Anthony, Appl. Phys. Lett. **89**, 192113 (2006).
[6] D. G. Cooke, F. A. Hegmann, Y. I. Mazur, W. Q. Ma, X. Wang, Z. M. Wang, G. J. Salamo, M. Xiao, T. D. Mishima, and M. B. Johnson, Appl. Phys. Lett. **85**, 3839 (2004).
[7] J. A. Fagan *et al.*, Phys. Rev. Lett. **98**, 147402 (2007).
[8] Y. Murakami, E. Einarsson, T. Edamura, and S. Maruyama, Phys. Rev. Lett. **94**, 087402 (2005).
[9] Y. Kim, N. Minami, and S. Kazaoui, Appl. Phys. Lett. **86**, 073103 (2005).
[10] G. S. Duesberg, I. Loa, M. Burghard, K. Syassen, and S. Roth, Phys. Rev. Lett. **85**, 5436 (2000).
[11] A. Nish, R. J. Nicholas, C. Faugeras, Z. Bao, and M. Potemski, Phys. Rev. B **78**, 245413 (2008).
[12] L. Ren, C. L. Pint, L. G. Booshenri, W. D. Rice, X. F. Wang, D. J. Hilton, K. Takeya, I. Kawayama, M. Tonouchi, R. H. Hauge, and J. Kono, Nano Lett. **9**, 2610 (2009).
[13] A. Jorio *et al.*, Phys. Rev. B **65**, 121402 (2002).
[14] T. I. Jeon, K. J. Kim, C. Kang, I. H. Maeng, J. H. Son, K. H. An, J. Y. Lee, and Y. H. Lee, J. Appl. Phys. **95**, 5736 (2004).
[15] H. Nishimura, N. Minami, and R. Shimano, Appl. Phys. Lett. **91**, 011108 (2007).
[16] L. Lüer, S. Hoseinkhani, D. Polli, J. Crochet, T. Hertel, and G. Lanzani, Nat. Phys. **5**, 54 (2009).
[17] O. J. Korovyanko, C. X. Sheng, Z. V. Vardeny, A. B. Dalton, and R. H. Baughman, Phys. Rev. Lett. **92**, 017403 (2004).
[18] S. Reich, M. Dworzak, A. Hoffmann, C. Thomsen, and M. S. Strano, Phys. Rev. B **71**, 033402 (2005).
[19] L. B. Huang, H. N. Pedrosa, and T. D. Krauss, Phys. Rev. Lett. **93**, 017403 (2004).
[20] S. M. Bachilo, M. S. Strano, C. Kittrell, R. H. Hauge, R. E. Smalley, and R. B. Weisman, Science **298**, 2361 (2002).
[21] P. Parkinson, J. Lloyd-Hughes, Q. Gao, H. H. Tan, C. Jagadish, M. B. Johnston, and L. M. Herz, Nano Lett. **7**, 2162 (2007).
[22] Y. Hashimoto, Y. Murakami, S. Maruyama, and J. Kono, Phys. Rev. B **75**, 245408 (2007).
[23] P. G. Collins, K. Bradley, M. Ishigami, and A. Zettl, Science **287**, 1801 (2000).
[24] A. Nish, J. Y. Hwang, J. Doig, and R. J. Nicholas, Nat. Nanotechnol. **2**, 640 (2007).
[25] X. Xu, K. Chuang, R. J. Nicholas, M. B. Johnston, and L. M. Herz, J. Phys. Chem. C **113**, 18106 (2009).
[26] M. F. Islam, D. E. Milkie, C. L. Kane, A. G. Yodh, and J. M. Kikkawa, Phys. Rev. Lett. **93**, 037404 (2004).
[27] S. Kilina, S. Tretiak, S. K. Doorn, Z. Luo, F. Papadimitrakopoulos, A. Piryatinski, A. Saxena, and A. R. Bishop, Proc. Natl. Acad. Sci. U.S.A. **105**, 6797 (2008).
[28] L. Perfetti, T. Kampfrath, F. Schapper, A. Hagen, T. Hertel, C. M. Aguirre, P. Desjardins, R. Martel, C. Frischkorn, and M. Wolf, Phys. Rev. Lett. **96**, 027401 (2006).
[29] J. S. Lauret, C. Voisin, G. Cassabois, C. Delalande, P. Roussignol, O. Jost, and L. Capes, Phys. Rev. Lett. **90**, 057404 (2003).
[30] C. Manzoni, A. Gambetta, E. Menna, M. Meneghetti, G. Lanzani, and G. Cerullo, Phys. Rev. Lett. **94**, 207401 (2005).